Nontrivial torque generation by orbital angular momentum injection in ferromagnetic-metal/Cu/Al₂O₃ trilayers

Junyeon Kim,[1,*] Dongwook Go,[2,3,4,5] Hanshen Tsai,[1,6] Daegeun Jo,[2] Kouta Kondou,[1]
Hyun-Woo Lee,[2,7,†] and YoshiChika Otani[1,6,‡]

[1]*Center for Emergent Matter Science, RIKEN, Wako, Saitama 351-0198, Japan*
[2]*Deparment of Physics, Pohang University of Science and Technology, Pohang 37673, Korea*
[3]*Basic Science Research Institute, Pohang University of Science and Technology, Pohang 37673, Korea*
[4]*Peter Grünberg Institut and Institute for Advanced Simulation, Forschungszentrum Jülich and JARA, 52428 Jülich, Germany*
[5]*Institute of Physics, Johannes Gutenberg University Mainz, 55099 Mainz, Germany*
[6]*Institute for Solid State Physics, The University of Tokyo, Kashiwa, Chiba 277–8581, Japan*
[7]*Asia Pacific Center for Theoretical Physics, Pohang 37673, Korea*

Efficient electrical generation of torque is desired to develop innovative magnetic nanodevices. The torque can be generated by charge to spin conversion of heavy-metal layers through their strong spin-orbit interaction followed by the injection of the converted spin into adjacent ferromagnetic layers. However heavy atomic elements indispensable for this torque generation scheme are often incompatible with device mass production processes. Here we demonstrate efficient torque generation without heavy elements in ferromagnetic metal/Cu/Al₂O₃ trilayers. Despite the absence of heavy elements, their effective spin Hall conductivity can be one order of magnitude larger than those of heavy-metal based multilayers. Properties of the measured torque deviate from those of the spin-injection induced torque and are consistent instead with a recently proposed torque mechanism based on orbital angular momentum injection. Our results demonstrate a direction for magnetic nanodevices based on the orbital angular momentum injection.

Electrically generated torque allows for electrical control of magnetism, which provides a promising route to realizing magnetic nanodevices. So far, the torque generation has been achieved by injecting spins into ferromagnetic layers [Fig. 1(a)]. In the mechanism of such spin-injection induced torque, heavy elements with strong spin-orbit interaction (SOI) are indispensable since spins have to be prepared beforehand via the charge to spin conversion such as the spin Hall effect (SHE) or the Edelstein effect (EE) [1–4]. However, the use of heavy elements is problematic for device applications since they are often highly resistive [5–8] and/or incompatible with mass production processes. This motivates a search for alternative methods to generate torque without heavy elements. Recently, it has been theoretically proposed that not only spin injection but also the injection of the orbital angular momentum (OAM) into ferromagnets (FMs) can generate torque [Fig. 1(b)], which is called orbital torque (OT) [9]. Unlike spin, the OAM can be electrically generated even without the SOI at all by light atomic elements [10,11]. The OAM injected into a FM can be converted to spin through the SOI of the FM and this spin generates the OT [9]. Even for 3d FM with weak SOI, it was estimated [9] and later confirmed by first-principles calculation [25] that the resulting OT can be comparable to or even larger than the conventional

spin-injection induced torque since the electrically generated OAM current [Fig. 1(c)] by the orbital Hall effect [12] or the orbital EE [13] can be much larger than the corresponding spin current by heavy elements [11,12]. Therefore the OT opens a direction for highly efficient magnetic nanodevices. Here we report experimental evidence for highly efficient torque generation without heavy elements in FM/Cu/Al₂O₃ trilayers, of which properties are at odds with the spin-injection induced torque but instead agree with the OT. This result not only provides a way to circumvent heavy elements and widen material choices for device applications but also uncovers a physics of the OAM transport.

To measure the torque in the trilayers, we perform the spin-torque ferromagnetic resonance (ST-FMR) measurement [Fig. 2(a)]. Each resonance peak in an ST-FMR spectrum can be decomposed into a symmetric component S and an antisymmetric component A [Fig. 2(b)]. Whereas A arises jointly by the fieldlike component of the torque and the current-induced Oersted field H_{rf}, S arises solely from the dampinglike component of the torque. Thus, when the fieldlike torque is negligible, which is the case for our experiment [14], the dampinglike torque generation efficiency θ is given by [15]

$$\theta = \frac{S}{A} \frac{4\pi M_s e t_{FM} d_{Cu}}{\hbar} \left[1 + \frac{4\pi M_{eff}}{H_{ext}}\right]^{1/2}, \quad (1)$$

where $4\pi M_s$ and $4\pi M_{eff}$ are the saturation magnetization and effective saturation magnetization of the FM,

*junyeon.kim@riken.jp
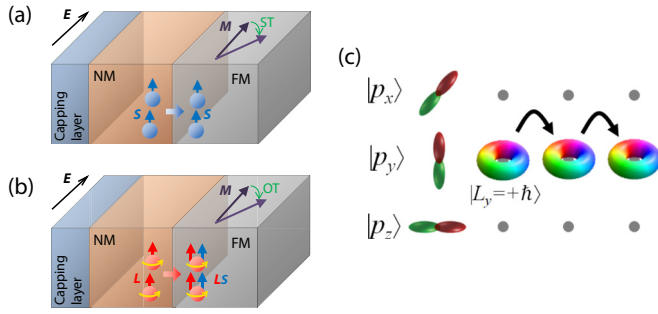†hwl@postech.ac.kr
‡yotani@issp.u-tokyo.ac.jp

FIG. 1. (a) The spin S (blue arrow) injection and (b) the OAM L (red arrow) injection from the NM to the FM for the spin-injection induced torque and the OT generation, respectively. (c) Through the orbital Hall effect or the orbital Rashba effect, an electron wave function may form superpositions such as $|L_y = +\hbar\rangle = (|p_z\rangle + i|p_x\rangle)/\sqrt{2}$, which carry nonzero OAM. The OAM current arises when electrons in such superposed states move to neighboring atoms.

respectively. e is the unit charge, $\hbar$ is the reduced Planck constant, t_{FM} is the thickness of the FM layer, d_{Cu} is the thickness of the Cu layer, and H_{ext} is the external field. We emphasize that θ in Eq. (1) includes contributions from both the spin injection and the OAM injection. For a $Co_{25}Fe_{75}$ (CoFe, 5 nm)/Cu(10 nm)/Al_2O_3 (20 nm) trilayer that does not contain any heavy element, we obtain $\theta \approx 0.12$, which is surprisingly high and comparable to those that utilize strong SHE of heavy elements [2,16]. We note that an additional voltage influenced by the spin pumping for the ST-FMR spectrum [17] is negligible in our trilayer since the damping enhancement by the spin pumping is vanishingly small, which is understandable since pumped spins cannot be absorbed in somewhere and thus are reflected entirely back to FM [14]. Still another source of the voltage is thermal effects through, for instance, the resonant heating [18]. However we estimate the thermal effects to be small since Cu is highly conductive and acts as a heat sink for CoFe [14]. On the other hand, the Edelstein magnetoresistance in a dc regime and the observation of the current-induced magnetization switching imply that θ is indeed large in our trilayer [14].

In addition to the unexpectedly large θ, the trilayer system exhibits interesting variation of θ when the FM in the trilayer
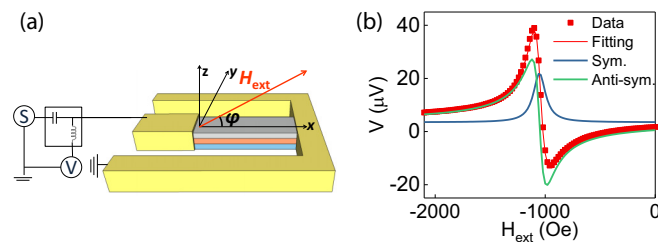

FIG. 2. (a) Experimental setup for the ST-FMR measurement. (b) Typical ST-FMR spectrum under 11 GHz-20-dBm rf source current from a device with $d_{Cu} = 9.8$ nm of CoFe/Cu/Al_2O_3. Red dot is the experimental data. Red, blue, and green lines are the fitting curve of the data, and its symmetric and antisymmetric components, respectively.
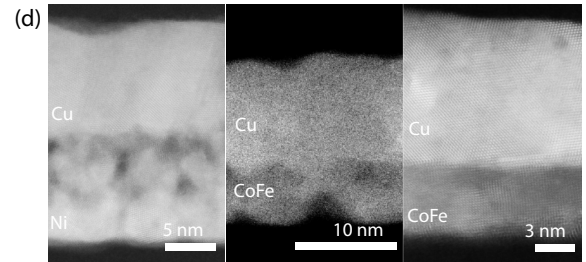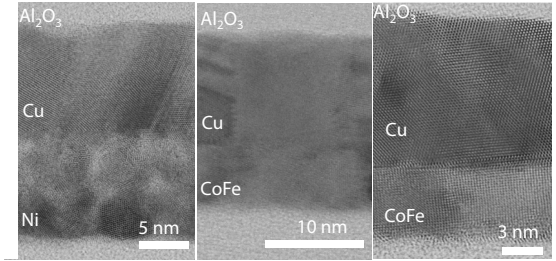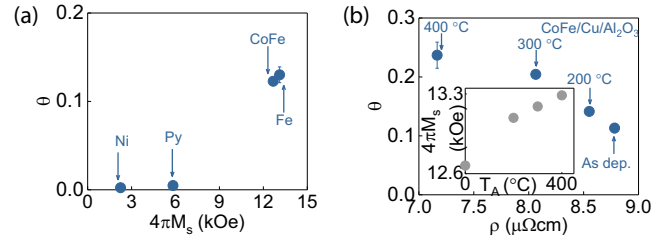

FIG. 3. (a) FM layer dependence of θ as a function of $4\pi M_s$. (b) Annealing temperature dependence of θ from the CoFe/Cu/Al_2O_3 structure as a function of resistivity ρ. Inset: $4\pi M_s$ for the whole sample as a function of the annealing temperature. Cross-sectional (c) bright-field STEM and (d) HAADF-STEM images for Ni/Cu/Al_2O_3 (left) as-deposited CoFe/Cu/Al_2O_3 (middle), and 300 °C annealed CoFe/Cu/Al_2O_3 (right).

is replaced by other $3d$ FMs such as Fe, $Ni_{80}Fe_{20}$ (Py), or Ni. In the modified trilayers, the thickness of the FM layer is chosen to 5 nm for Fe and Py, but to a larger value 12 nm for Ni since it has smaller $4\pi M_s$ and $4pM_{eff}$ than the other FMs. The ST-FMR measurement for the modified trilayers indicates that θ varies about two orders of magnitude depending on the FM material choice: $\theta \approx 0.12$ for CoFe, ~ 0.13 for Fe, ~ 0.005 for Py, and ~ 0.002 for Ni [Fig. 3(a)]. Such a wide variation of θ is unusual in spin-injection systems where θ is determined mainly by the spin source material choice (heavy metals) and affected much weakly by the FM material choice (within a factor of 4) [19]. Spin-injection systems can exhibit such a wide variation of θ if the spin-mixing conductance or the spin memory loss varies much with FM. To test this possibility, we prepare a set of reference trilayers FM/Cu/Bi_2O_3, where the spin-injection induced torque arises due to the EE at the Cu/Bi_2O_3 interface that contains the heavy element Bi. It turns out that the values of θ for the reference trilayers are roughly the same ($0.02 \leqslant \theta \leqslant 0.04$) regardless of the FM material choice (FM = CoFe, Fe, Py, and Ni), implying that the spin-mixing conductance or the spin memory loss does not vary much with the FM material choice [14]. Thus, the surprisingly large variation of θ with the FM material choice

only for the original trilayers is hard to explain within the spin-injection picture and we conclude that the mechanisms of the torque are different in the two types of trilayers. As a passing remark, we mention that the spin pumping is strong for the reference trilayers [14], implying that pumped spins can be absorbed near the Cu/Bi_2O_3 interface [20–23]. Thus, the values of θ for the reference trilayers given above are obtained after the measured ST-FMR spectra are corrected to take into account the spin-pumping effect [17]. This is another contrast with the original trilayers, where the spin pumping is negligible.

To explain the results for the original trilayers, one needs a mechanism that can generate a large torque without strong SOI. A recent theory reported that sizable spin currents can be generated *internally* within 3d FMs [24]. However the predicted spin Hall conductivities and anomalous spin Hall conductivities for Ni are of the same order as the corresponding values for Fe and thus cannot explain two orders of magnitude different θ values for Ni and Fe in our experiment.

The OAM injection from a normal metal with negligible SOI into a 3d FM can also generate large torques [9,25]. The strength of this OT mechanism depends on the FM material choice in two ways. One is the SOI strength of a FM but this factor cannot explain two orders of magnitude difference in the observed θ values since the SOI strength of various 3d FMs are not that much different from each other. The other is the quality of the interface through which the OAM is injected (FM/Cu interface in our trilayers). It was argued [9] that the OAM transport is more vulnerable to the interfacial disorder than the spin transport is and thus the efficiency of the OT mechanism is more sensitive to the interface quality than the efficiency of spin injection mechanisms is. In this respect, it is interesting that Ni and Cu are notorious for their intermixing at the Ni/Cu interface whereas the Co (or Fe) and Cu are known to get segregated spontaneously and form a well-ordered Co (or Fe)/Cu interface [26]. Thus, the interface sensitivity of the OT mechanism provides a possible way to explain the large difference between the large θ group (CoFe and Fe) and the small θ group (Ni and Py).

To examine this possibility, we probe the interface quality by the cross-sectional bright-field scanning transmission electron microscope (bright field-STEM) [Fig. 3(c)] and high-angle annular dark-field STEM (HAADF-STEM) [Fig. 3(d)]. The resulting images clearly indicate significant intermixing at the Ni/Cu interface [left panels in Figs. 3(c) and 3(d)] and much better ordered CoFe/Cu interface [middle panels in Figs. 3(c) and 3(d)]. Thus, the θ variation is indeed correlated with the degree of the interface quality at the FM/Cu interface. To examine the correlation further, we fix the FM to CoFe and anneal CoFe (5 nm)/Cu (12 nm)/Al_2O_3 (20 nm) trilayers at different temperatures [Fig. 3(c)]. Since both Co and Fe tend to get segregated from Cu, the CoFe/Cu interface quality is expected to improve upon annealing. The bright-field-STEM and HAADF-STEM images of the as-deposited trilayer [middle panels in Figs. 3(c) and 3(d)] and the trilayer annealed at 300 °C [right panels in Figs. 3(c) and 3(d)] show that the interface quality is indeed enhanced upon annealing, which is consistent with the previous report [27]. In concurrence with this change, θ grows from ~0.12 to ~0.24 [Fig. 3(b)], verifying the correlation between θ and the interface quality
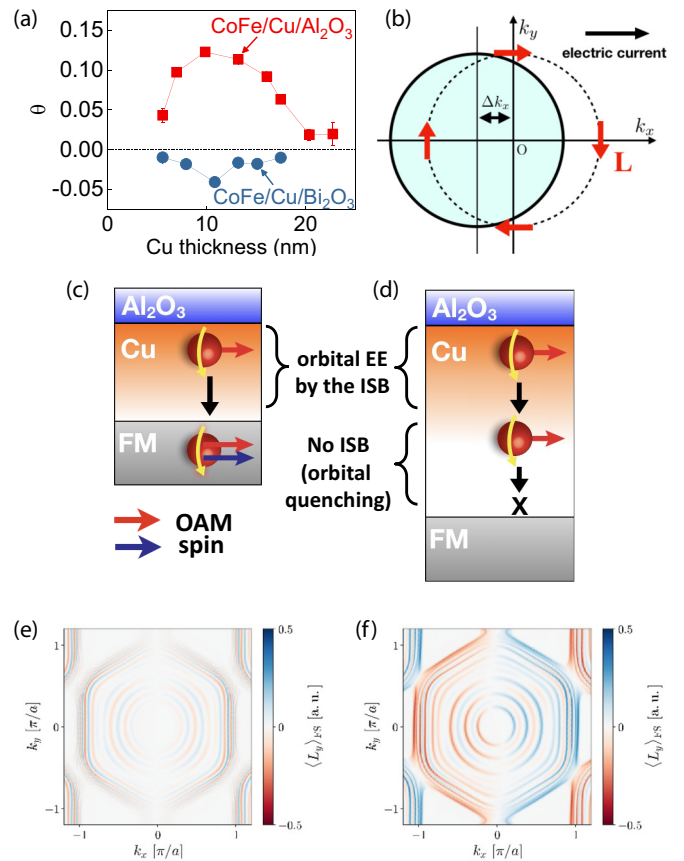

FIG. 4. (a) Cu thickness (d_{Cu}) dependence of θ for the CoFe/Cu/Al_2O_3 (red square) and the CoFe/Cu/Bi_2O_3 (blue circle). (b) Generation of the OAM by the orbital EE. Schematic illustrations of the orbital transport in FM/Cu/Al_2O_3 trilayer for (c) thin and (d) thick Cu samples. OAM textures for Cu films (e) without and (f) with the inversion symmetry breaking, respectively.

further. It is worth mentioning that the annealing lowers the resistance of the trilayer [Fig. 3(b)], which is understandable since the interfacial scattering at disordered interfaces is an important source of the resistance in thin films. We emphasize that this correlation between θ and the interface quality cannot be explained by the spin-injection induced torque since the spin-mixing conductance is affected very weakly ($<5\%$) by the intermixing at the 3d FM/Cu interface [28] and the spin memory loss stays weak in systems without heavy elements. Moreover our experimental result is in stark contrast with the *enhancement* of θ by the intermixing for a Co/Pt bilayer [29], for which the conventional spin-injection induced torque is the dominant source of the torque.

Next we discuss roles of Cu/Al_2O_3 within the FM/Cu/Al_2O_3 trilayers with regard to the OT mechanism. One obvious role is to generate the OAM flow [Figs. 4(c) and 4(d)]. The clear difference from the reference trilayers FM/Cu/Bi_2O_3 indicates that the OAM flow is generated at the Cu/Al_2O_3 interface or in the upper part of the Cu layer close to the interface, which may be affected by the Al_2O_3 layer through some kind of "proximity" effect. In principle, the OAM flow can be generated also within the Cu layer itself (without the help of the proximity effect) through the orbital Hall effect. However the calculated orbital Hall

conductivity of pristine Cu [12] is insufficient to explain the large value of θ for the FM/Cu/Al$_2$O$_3$ trilayers. The difference between the original and the reference trilayers also supports a negligible role of the Cu layer. We thus attribute the OAM flow generation to the orbital EE [13], which is the OAM counterpart of the spin EE. Since the orbital EE does not require the SOI and arises from the combination of the inversion symmetry breaking and an electric current flow, the Cu/Al$_2$O$_3$ interface is a natural location where the orbital EE occurs. When the interface lies in the xy plane and an electrical current is applied along the x direction, the orbital EE generates the y-polarized OAM density [Fig. 4(b)], which can diffuse and be injected to the FM to generate the dampinglike torque measured by the ST-FMR.

In this theoretical picture, the Cu layer in the original trilayers acts mainly as the OAM transport channel from the OAM source (the Cu/Al$_2$O$_3$ interface or the proximity region) to the OAM target (FM). We examine experimentally the OAM transport in the Cu layer through the Cu layer thickness (d_{Cu}) dependence of θ. The basic idea is that the OT will be suppressed if the Cu layer is sufficiently thicker than the OAM relaxation length in Cu. Although the OAM relaxation length has not been evaluated before to the best of our knowledge, it is reasonable to expect that the OAM relaxation length in Cu is much shorter than the spin relaxation length in Cu ($\sim$0.5 μm at room temperature [30]) since the crystal field in Cu tends to suppress the OAM (OAM quenching). As shown in Fig. 4(a), θ for the CoFe/Cu/Al$_2$O$_3$ trilayer decreases by a factor of 6 from 0.012 to 0.02 as the Cu layer thickness d_{Cu} grows from 10 to 22 nm. It exceeds an expectation based on the trend of the spin-injection induced torque as supported by θ for the reference trilayer CoFe/Cu/Bi$_2$O$_3$ [Fig. 4(a)]. We thus conclude that for the CoFe/Cu/Al$_2$O$_3$ trilayer, the d_{Cu} dependence of θ is inconsistent with the spin injection but in agreement with the OAM injection. The current shunting can result in partial decrease in θ but this effect is weak to explain the factor of 6 decrease.

Recently, efficient torque generation was observed in a FM/(surface-oxidized Cu) bilayer structure [31–33]. It was theoretically suggested [33] that the oxidation level gradient along the Cu thickness direction can generate a vortex pattern in the in-plane electric current-density distribution in the Cu layer and the vortex generates a spin current through the vortex-spin coupling. It is in principle possible that the Cu layer in our FM/Cu/Al$_2$O$_3$ trilayers is also surface oxidized through the diffusion of oxygen atoms from the Cu/Al$_2$O$_3$ interface as shown in the x-ray photoemission spectroscopy (XPS) observation [14]. However, we estimate that the level of the surface oxidization in the Cu layer is weaker in our trilayers compared to the previous experiments [31–33] as supported by lower Cu resistivity (for 10 nm of layer thickness, $\sim$9.4 $\mu\Omega$ cm in our Cu layer, but $\sim$14 $\mu\Omega$ cm in oxidized Cu layer in Ref. [33]). Moreover, the spin-injected mechanism cannot explain the drastic FM dependence of θ for the FM/Cu/Al$_2$O$_3$ trilayers. We also note that θ is much smaller for our Py/Cu/Al$_2$O$_3$ trilayer (0.005) than the Py/surface-oxidized Cu bilayer (0.08 [31] and 0.03 [33]). Thus we conclude that the spin current generation mechanism in Ref. [33] is not important in our trilayers. On the other hand, we cannot rule out the possibility that the oxidation level

gradient in the Cu layer generates the OAM current. When the inversion symmetry is broken (by the oxidation level gradient in the upper part of the Cu layer), the orbital quenching is lifted and energy eigenstates acquire nonzero OAM whose direction depends on the crystal momentum [10,34,35]. This orbital Rashba effect [Figs. 4(e) and 4(f)] provides a natural platform for the orbital EE [13] in the upper part of the Cu layer [Fig. 4(d)] and also provides a possible explanation for the increase of θ as d_{Cu} increases from 5 to 10 nm [Fig. 4(a)]. Figures 4(c) and 4(d) summarize the revised theoretical picture for the OT mechanism in the FM/Cu/Al$_2$O$_3$ trilayers. Both the Cu/Al$_2$O$_3$ interface and the "proximity" region of the Cu layer (oxidation level gradient) act as the OAM source whereas the pristine Cu layer (lower part of the Cu layer) acts as the OAM transport channel.

A few remarks are in order. The orbital Rashba effect and the orbital EE are possible also near the FM/Cu interface [35], where the inversion symmetry is broken. However, the clear difference between the FM/Cu/Al$_2$O$_3$ trilayers and the FM/Cu/Bi$_2$O$_3$ trilayers despite the common presence of the FM/Cu interface in both types of the trilayers indicates that the inversion symmetry breaking near the FM/Cu interface is not important. The orbital Rashba effect and the orbital EE are possible also near the Cu/Bi$_2$O$_3$ interface. But we do not find any evidence for those effects in the FM/Cu/Bi$_2$O$_3$ trilayers. One possible reason is that the inversion symmetry breaking is weak at the Cu/Bi$_2$O$_3$ interface since the work function difference at the Cu/Bi$_2$O$_3$ interface is only 0.05 eV [22], which is smaller than the work function difference of 0.24 eV at the Cu/Al$_2$O$_3$ interface. The oxidation level gradient near the Cu/Bi$_2$O$_3$ interface is also found to be weaker than that near the Cu/Al$_2$O$_3$ interface according to the XPS measurement [14]. We find weak correlation between θ and the saturation magnetization M_S. As shown in Fig. 3(a), $4\pi M_S$ for the FM layer in the FM/Cu/Al$_2$O$_3$ trilayers is larger for FM = CoFe and Fe with larger θ and smaller for FM = Ni and Py with much smaller θ. The annealing temperature dependence of θ for the CoFe/Cu/Al$_2$O$_3$ trilayer also shows the positive correlation between θ and $4\pi M_S$. [Fig. 3(b) inset].

Finally, we remark on the technological aspects of the OT device application. Observation of gigantic efficiency $\theta \approx 0.24$ [Fig. 3(c)] in CoFe/Cu/Al$_2$O$_3$ is close to the value for device structures that utilize the strong SHE of β-phase W, which has the largest spin Hall angle among single-elemental metallic materials [5,7]. Particularly, the "effective" spin Hall conductivity σ_s, which is defined by $\sigma_s = (\hbar/2e)\sigma\theta$, where σ is the charge conductivity, is at least 3.4 $\times$ 10^4 $(\hbar/2e)$ Ω^{-1} cm^{-1} for 400 °C annealed CoFe/Cu/Al$_2$O$_3$ trilayer. It is more than 10 times larger than those of heavy elements such as fcc Pt [36] and β-phase W [37], and about 100 times larger than that of topological insulators [38]. Note that the σ_s value is obtained assuming perfect interface transparency, thus its actual value can be even larger. Thanks to low resistivity (5 $\sim$ 10 $\mu\Omega$ cm) of Cu, it offers energy-efficient device operation, which guarantees endurance against repetitive cycles by lowering the Joule heating [39].

In summary, we find a large torque in CoFe/Cu/Al$_2$O$_3$ trilayers which do not contain any heavy element. The CoFe/Cu/Al$_2$O$_3$ trilayers show extremely large spin Hall conductivity. Also we find the anomalous torque dependences

on the ferromagnetic material selection and the annealing temperature, which are in clear contrast to the torque that arises from the spin injection. All these behaviors are well understood if we consider the unique property of the OAM transport and the OT mechanism. Our result reveals a highly efficient and energy-friendly orbitronic platform for torque device applications.

[1] I. M. Miron, K. Garello, G. Gaudin, P.-J. Zermatten, M. V. Costache, S. Auffret, S. Bandiera, B. Rodmacq, A. Schuhl, and P. Gambardella, Nature (London) **476**, 189 (2011).

[2] L. Liu, C.-F. Pai, Y. Li, H. W. Tseng, D. C. Ralph, and R. A. Buhrman, Science **336**, 555 (2012).

[3] A. R. Mellnik, J. S. Lee, A. Richardella, J. L. Grab, P. J. Mintun, M. H. Fischer, A. Vaezi, A. Manchon, E.-A. Kim, N. Samarth, and D. C. Ralph, Nature (London) **511**, 449 (2014).

[4] J. C. R. Sánchez, L. Vila, G. Desfonds, S. Gambarelli, J. P. Attané, J. M. De Teresa, C. Magén, and A. Fert, Nat. Commun. **4**, 2944 (2013).

[5] C.-F. Pai, L. Liu, Y. Li, H. W. Tseng, D. C. Ralph, and R. A. Buhrman, Appl. Phys. Lett. **101**, 122404 (2012).

[6] J. Kim, J. Sinha, S. Mitani, M. Hayashi, S. Takahashi, S. Maekawa, M. Yamanouchi, and H. Ohno, Phys. Rev. B **89**, 174424 (2014).

[7] J. Kim, P. Sheng, S. Takahashi, S. Mitani, and M. Hayashi, Phys. Rev. Lett. **116**, 097201 (2016).

[8] K.-U. Demasius, T. Phung, W. Zhang, B. P. Hughes, S.-H. Yang, A. Kellock, W. Han, A. Pushp, and S. S. P. Parkin, Nat. Commun. **7**, 10644 (2016).

[9] D. Go and H.-W. Lee, Phys. Rev. Research **2**, 013177 (2020).

[10] S. R. Park, C. H. Kim, J. Yu, J. H. Han, and C. Kim, Phys. Rev. Lett. **107**, 156803 (2011).

[11] D. Go, D. Jo, C. Kim, and H.-W. Lee, Phys. Rev. Lett. **121**, 086602 (2018).

[12] D. Jo, D. Go, and H.-W. Lee, Phys. Rev. B **98**, 214405 (2018).

[13] A. Johansson, B. Göbel, J. Henk, M. Bibes, and I. Mertig, arXiv:2006.14958.

[14] See Supplemental Material at http://link.aps.org/supplemental/10.1103/PhysRevB.103.L020407 for details of the theoretical assertions, sample preparation, various spin response measurement techniques including ST-FMR, Edelstein magnetoresistance, spin pumping, magnetization switching, and material characterization, which includes Refs. [3,9–12,17,18,21,22,40–57].

[15] L. Liu, T. Moriyama, D. C. Ralph, and R. A. Buhrman, Phys. Rev. Lett. **106**, 036601 (2011).

[16] K. Kondou, H. Sukegawa, S. Mitani, K. Tsukagoshi, and S. Kasai, Appl. Phys. Express **5**, 073002 (2012).

[17] K. Kondou, H. Sukegawa, S. Kasai, S. Mitani, Y. Niimi, and Y. Otani, Appl. Phys. Express **9**, 023002 (2016).

[18] S. Karimeddiny, J. A. Mittelstaedt, R. A. Buhrman, and D. C. Ralph, Phys. Rev. Appl. **14**, 024024 (2020).

[19] W. Zhang, W. Han, X. Jiang, S.-H. Yang, and S. S. P. Parkin, Nat. Phys. **11**, 496 (2015).

[20] S. Karube, K. Kondou, and Y. Otani, Appl. Phys. Express **9**, 033001 (2016).

[21] J. Kim, Y.-T. Chen, S. Karube, S. Takahashi, K. Kondou, G. Tatara, and Y. C. Otani, Phys. Rev. B **96**, 140409(R) (2017).

[22] H. Tsai, S. Karube, K. Kondou, N. Yamaguchi, F. Ishii, and Y. Otani, Sci. Rep. **8**, 5564 (2018).

[23] M. Xu, J. Puebla, F. Auvray, B. Rana, K. Kondou, and Y. Otani, Phys. Rev. B **97**, 180301(R) (2018).

[24] V. P. Amin, J. Li, M. D. Stiles, and P. M. Haney, Phys. Rev. B **99**, 220405(R) (2019).

[25] D. Go, F. Freimuth, J.-P. Hanke, F. Xue, O. Gomonay, K.-J. Lee, S. Blugel, P. M. Haney, H.-W. Lee, and Y. Mokrousov, Phys. Rev. Research **2**, 033401 (2020).

[26] S. S. P. Parkin, Phys. Rev. Lett. **71**, 1641 (1993).

[27] M. Menyhard, A. Sulyok, K. Pentek, and A. M. Zeltser, Thin Solid Films **366**, 129 (2000).

[28] M. Zwierzycki, Y. Tserkovnyak, P. J. Kelly, A. Brataas, and G. E. W. Bauer, Phys. Rev. B **71**, 064420 (2005).

[29] L. Zhu, D. C. Ralph, and R. A. Buhrman, Phys. Rev. B **99**, 180404(R) (2019).

[30] T. Kimura, T. Sato, and Y. Otani, Phys. Rev. Lett. **100**, 066602 (2008).

[31] H. An, Y. Kageyama, Y. Kanno, N. Enishi, and K. Ando, Nat. Commun. **7**, 13069 (2016).

[32] T. Gao, A. Qaiumzadeh, H. An, A. Musha, Y. Kageyama, J. Shi, and K. Ando, Phys. Rev. Lett. **121**, 017202 (2018).

[33] G. Okano, M. Matsuo, Y. Ohnuma, S. Maekawa, and Y. Nozaki, Phys. Rev. Lett. **122**, 217701 (2019).

[34] B. Kim, C. H. Kim, P. Kim, W. Jung, Y. Kim, Y. Koh, M. Arita, K. Shimada, H. Namatame, M. Taniguchi, J. Yu, and C. Kim, Phys. Rev. B **85**, 195402 (2012).

[35] J.-H. Park, C. H. Kim, J.-W. Rhim, and J. H. Han, Phys. Rev. B **85**, 195401 (2012).

[36] G. Y. Guo, S. Murakami, T. W. Chen, and N. Nagaosa, Phys. Rev. Lett. **100**, 096401 (2008).

[37] E. Derunova, Y. Sun, C. Felser, S. S. P. Parkin, B. Yan, and M. N. Ali, Sci. Adv. **5**, eaav8575 (2019).

[38] M. DC, R. Grassi, J.-Y. Chen, M. Jamali, D. R. Hickey, D. Zhang, Z. Zhao, H. Li, P. Quarterman, Y. Lv, M. Li, A. Manchon, K. A. Mkhoyan, T. Low, and J.-P. Wang, Nat. Mater. **17**, 800 (2018).

[39] S. Fukami, T. Anekawa, C. Zhang, and H. Ohno, Nat. Nanotechnol. **11**, 621 (2016).

[40] H. Kontani, T. Tanaka, D. S. Hirashima, K. Yamada, and J. Inoue, Phys. Rev. Lett. **102**, 016601 (2009).

[41] T. Tanaka, H. Kontani, M. Naito, T. Naito, D. S. Hirashima, K. Yamada, and J. Inoue, Phys. Rev. B **77**, 165117 (2008).

[42] D. A. Papaconstantopoulos, *Handbook of the Band Structure of Elemental Solids: From Z = 1 to Z = 112*, 2nd ed. (Springer, New York, 2015).

[43] K. V. Shanavas, Z. S. Popović, and S. Satpathy, Phys. Rev. B **90**, 165108 (2014).

[44] H. Ishida, Phys. Rev. B **90**, 235422 (2014).

[45] J.-H. Park, C. H. Kim, H.-W. Lee, and J. H. Han, Phys. Rev. B **87**, 041301(R) (2013).

[46] C.-F. Pai, Y. Ou, L. H. Vilela-Leão, D. C. Ralph, and R. A. Buhrman, Phys. Rev. B **92**, 064426 (2015).

[47] O. Mosendz, V. Vlaminck, J. E. Pearson, F. Y. Fradin, G. E. W. Bauer, S. D. Bader, and A. Hoffmann, Phys. Rev. B **82**, 214403 (2010).

[48] S. Zhang and A. Fert, Phys. Rev. B **94**, 184423 (2016).

[49] R. Dey, N. Prasad, L. F. Register, and S. K. Banerjee, Phys. Rev. B **97**, 174406 (2018).

[50] H. Nakayama, Y. Kanno, H. An, T. Tashiro, S. Haku, A. Nomura, and K. Ando, Phys. Rev. Lett. **117**, 116602 (2016).

[51] G. Mihajlović, O. Mosendz, L. Wan, N. Smith, Y. Choi, Y. Wang, and J. A. Katine, Appl. Phys. Lett. **109**, 192404 (2016).

[52] W. Gil, D. Görlitz, M. Horisberger, and J. Kötzler, Phys. Rev. B **72**, 134401 (2005).

[53] D. Fang, H. Kurebayashi, J. Wunderlich, K. Vyborny, L. P. Zarbo, R. P. Campion, A. Casiraghi, B. L. Gappagher, T. Jungwirth, and A. J. Ferguson, Nat. Nanotechnol. **6**, 413 (2011).

[54] K.-D. Lee, D.-J. Kim, H. Y. Yoon, S.-H. Kim, J.-H. Lee, K.-M. Lee, J.-R. Jeong, K.-S. Lee, H.-S. Song, J.-W. Sohn, S.-C. Shin, and B.-G. Park, Sci. Rep. **5**, 10249 (2015).

[55] M. Harder, Z. X. Cao, Y. S. Gui, X. L. Fan, and C. M. Hu, Phys. Rev. B **84**, 054423 (2011).

[56] L. Zhu, D. C. Ralph, and R. A. Buhrman, Phys. Rev. Lett. **123**, 057203 (2019).

[57] M. A. W. Schoen, D. Thonig, M. L. Schneider, T. J. Silva, H. T. Nembach, O. Eriksson, O. Karis, and J. M. Shaw, Nat. Phys. **12**, 839 (2016).